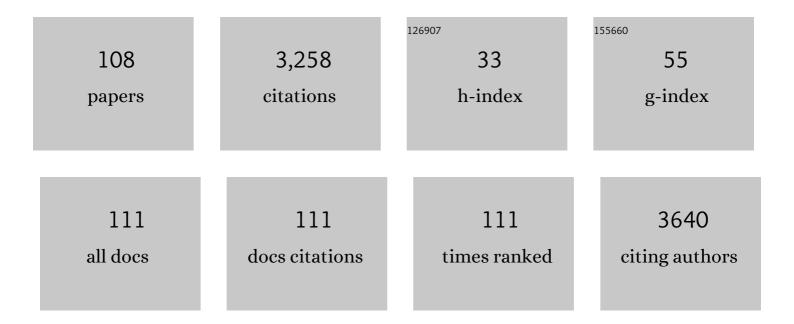
Adam M Alessio

List of Publications by Year in descending order

Source: https://exaly.com/author-pdf/8794838/publications.pdf Version: 2024-02-01



#	Article	IF	CITATIONS
1	What are the basic concepts of temporal, contrast, and spatial resolution in cardiac CT?. Journal of Cardiovascular Computed Tomography, 2009, 3, 403-408.	1.3	214
2	The impact of respiratory motion on tumor quantification and delineation in static PET/CT imaging. Physics in Medicine and Biology, 2009, 54, 7345-7362.	3.0	208
3	Application and Evaluation of a Measured Spatially Variant System Model for PET Image Reconstruction. IEEE Transactions on Medical Imaging, 2010, 29, 938-949.	8.9	189
4	Modeling and incorporation of system response functions in 3-D whole body PET. IEEE Transactions on Medical Imaging, 2006, 25, 828-837.	8.9	156
5	Quantification of Myocardial Blood Flow inÂAbsolute Terms Using 82Rb PET Imaging. JACC: Cardiovascular Imaging, 2014, 7, 1119-1127.	5.3	144
6	Weight-Based, Low-Dose Pediatric Whole-Body PET/CT Protocols. Journal of Nuclear Medicine, 2009, 50, 1570-1578.	5.0	108
7	Pediatric CT: Strategies to Lower Radiation Dose. American Journal of Roentgenology, 2013, 200, 950-956.	2.2	104
8	Tumor delineation using PET in head and neck cancers: Threshold contouring and lesion volumes. Medical Physics, 2006, 33, 4280-4288.	3.0	100
9	Quiescent period respiratory gating for PET/CT. Medical Physics, 2010, 37, 5037-5043.	3.0	94
10	Cine CT for Attenuation Correction in Cardiac PET/CT. Journal of Nuclear Medicine, 2007, 48, 794-801.	5.0	93
11	Image reconstruction for PET/CT scanners: past achievements and future challenges. Imaging in Medicine, 2010, 2, 529-545.	0.0	89
12	Ultra-low dose CT attenuation correction for PET/CT. Physics in Medicine and Biology, 2012, 57, 309-328.	3.0	84
13	Performance evaluation of the $5\hat{a}\in R$ ing GE Discovery MI PET/CT system using the national electrical manufacturers association NU $2\hat{a}\in 2012$ Standard. Medical Physics, 2019, 46, 3025-3033.	3.0	78
14	Comparison Between Pre-Log and Post-Log Statistical Models in Ultra-Low-Dose CT Reconstruction. IEEE Transactions on Medical Imaging, 2017, 36, 707-720.	8.9	77
15	Model-Based Iterative Reconstruction Versus Adaptive Statistical Iterative Reconstruction and Filtered Back Projection in Liver 64-MDCT: Focal Lesion Detection, Lesion Conspicuity, and Image Noise. American Journal of Roentgenology, 2013, 200, 1071-1076.	2.2	71
16	PET/CT scanner instrumentation, challenges, and solutions. Radiologic Clinics of North America, 2004, 42, 1017-1032.	1.8	65
17	Respiratory motion correction for quantitative PET/CT using all detected events with internal-external motion correlation. Medical Physics, 2011, 38, 2715-2723.	3.0	64
18	Quantifying and Reducing the Effect of Calibration Error on Variability of PET/CT Standardized Uptake Value Measurements. Journal of Nuclear Medicine, 2011, 52, 218-224.	5.0	62

#	Article	IF	CITATIONS
19	Prospective Trial Using Internal Pair-Production Positron Emission Tomography to Establish the Yttrium-90 Radioembolization Dose Required for Response of Hepatocellular Carcinoma. International Journal of Radiation Oncology Biology Physics, 2018, 101, 358-365.	0.8	60
20	Properties and Mitigation of Edge Artifacts in PSF-Based PET Reconstruction. IEEE Transactions on Nuclear Science, 2011, 58, 2264-2275.	2.0	59
21	Quantitative material characterization from multiâ€energy photon counting CT. Medical Physics, 2013, 40, 031108.	3.0	55
22	Dual Energy CT Attenuation Correction Methods for Quantitative Assessment of Response to Cancer Therapy with PET/CT Imaging. Technology in Cancer Research and Treatment, 2006, 5, 319-327.	1.9	53
23	Improved quantitation for PET/CT image reconstruction with system modeling and anatomical priors. Medical Physics, 2006, 33, 4095-4103.	3.0	53
24	Comparison of blood flow models and acquisitions for quantitative myocardial perfusion estimation from dynamic CT. Physics in Medicine and Biology, 2014, 59, 1533-1556.	3.0	53
25	Optimization of Pediatric PET/CT. Seminars in Nuclear Medicine, 2017, 47, 258-274.	4.6	53
26	Comparison of Positron Emission Tomography and Bremsstrahlung Imaging to Detect Particle Distribution in Patients Undergoing Yttrium-90 Radioembolization for Large Hepatocellular Carcinomas or Associated Portal Vein Thrombosis. Journal of Vascular and Interventional Radiology, 2013, 24, 1147-1153.	0.5	44
27	CT Detectability of Small Low-Contrast Hypoattenuating Focal Lesions: Iterative Reconstructions versus Filtered Back Projection. Radiology, 2018, 289, 443-454.	7.3	42
28	Evaluation of Optimal Acquisition Duration or Injected Activity for Pediatric ¹⁸ F-FDG PET/CT. Journal of Nuclear Medicine, 2011, 52, 1028-1034.	5.0	41
29	Applying a patient-specific bio-mathematical model of glioma growth to develop virtual [18F]-FMISO-PET images. Mathematical Medicine and Biology, 2012, 29, 31-48.	1.2	41
30	Attenuationâ€emission alignment in cardiac PET/CT based on consistency conditions. Medical Physics, 2010, 37, 1191-1200.	3.0	40
31	Accuracy of CT-based attenuation correction in PET/CT bone imaging. Physics in Medicine and Biology, 2012, 57, 2477-2490.	3.0	40
32	A pediatric CT dose and risk estimator. Pediatric Radiology, 2010, 40, 1816-1821.	2.0	37
33	Improved prediction of lobar perfusion contribution using technetium-99m–labeled macroaggregate of albumin single photonÂemission computed tomography/computed tomography withÂattenuation correction. Journal of Thoracic and Cardiovascular Surgery, 2014, 148, 2345-2352.	0.8	35
34	Role of Reference Levels in Nuclear Medicine: A Report of the SNMMI Dose Optimization Task Force. Journal of Nuclear Medicine, 2015, 56, 1960-1964.	5.0	32
35	Accuracy of Myocardial Blood Flow Estimation From Dynamic Contrast-Enhanced Cardiac CT Compared With PET. Circulation: Cardiovascular Imaging, 2019, 12, e008323.	2.6	29
36	Multi-Objective Evolutionary Algorithm for PET Image Reconstruction: Concept. IEEE Transactions on Medical Imaging, 2021, 40, 2142-2151.	8.9	27

#	Article	IF	CITATIONS
37	Myocardial hypo-enhancement on resting computed tomography angiography images accurately identifies myocardial hypoperfusion. Journal of Cardiovascular Computed Tomography, 2011, 5, 412-420.	1.3	25
38	Resolution modeling enhances PET imaging. Medical Physics, 2013, 40, 120601.	3.0	25
39	High resolution FDG-microPET of carotid atherosclerosis: plaque components underlying enhanced FDG uptake. International Journal of Cardiovascular Imaging, 2016, 32, 145-152.	1.5	24
40	Effect of Reconstruction Algorithms on Myocardial Blood Flow Measurement with 13N-Ammonia PET. Journal of Nuclear Medicine, 2007, 48, 1259-1265.	5.0	23
41	A phantom design for assessment of detectability in PET imaging. Medical Physics, 2016, 43, 5051-5062.	3.0	20
42	Dual energy CT for attenuation correction with PET/CT. Medical Physics, 2013, 41, 012501.	3.0	19
43	Ovarian torsion: developing a machine-learned algorithm for diagnosis. Pediatric Radiology, 2020, 50, 706-714.	2.0	19
44	Role of Limited Whole-Body PET/CT in Pediatric Lymphoma. American Journal of Roentgenology, 2011, 196, 1047-1055.	2.2	18
45	Validation of an axially distributed model for quantification of myocardial blood flow using 13N-ammonia PET. Journal of Nuclear Cardiology, 2013, 20, 64-75.	2.1	17
46	Impact of CT attenuation correction method on quantitative respiratoryâ€correlated (4D) PET/CT imaging. Medical Physics, 2015, 42, 110-120.	3.0	17
47	Ultra-low dose CT attenuation correction for PET/CT: analysis of sparse view data acquisition and reconstruction algorithms. Physics in Medicine and Biology, 2015, 60, 7437-7460.	3.0	15
48	Estimated cumulative radiation dose from PET/CT in children with malignancies. Pediatric Radiology, 2010, 40, 1712-1713.	2.0	14
49	Hepatotoxic Dose Thresholds by Positron-Emission Tomography After Yttrium-90 Radioembolization of Liver Tumors: A Prospective Single-Arm Observational Study. CardioVascular and Interventional Radiology, 2018, 41, 1363-1372.	2.0	14
50	Multiscale modeling of metabolism, flows, and exchanges in heterogeneous organs. Annals of the New York Academy of Sciences, 2010, 1188, 111-120.	3.8	13
51	latrogenic Radiation Exposure to Patients With Early Onset Spine and Chest Wall Deformities. Spine, 2013, 38, E1108-E1114.	2.0	12
52	Comparison of Micro–Computed Tomography and Clinical Computed Tomography Protocols for Visualization of Nasal Cartilage Before Surgical Planning for Rhinoplasty. JAMA Facial Plastic Surgery, 2019, 21, 237-243.	2.1	12
53	Morphology supporting function: attenuation correction for SPECT/CT, PET/CT, and PET/MR imaging. Quarterly Journal of Nuclear Medicine and Molecular Imaging, 2016, 60, 25-39.	0.7	12
54	Application of a spatially variant system model for 3-D whole-body pet image reconstruction. , 2008, 2008, 1315-1318.		11

#	Article	IF	CITATIONS
55	MAP reconstruction from spatially correlated PET data. IEEE Transactions on Nuclear Science, 2003, 50, 1445-1451.	2.0	9
56	A study of SPECT/CT camera stability for quantitative imaging. EJNMMI Physics, 2016, 3, 14.	2.7	8
57	Sinogram smoothing techniques for myocardial blood flow estimation from dose-reduced dynamic computed tomography. Journal of Medical Imaging, 2014, 1, 034004.	1.5	7
58	Establishment of normative values for the fetal posterior fossa by magnetic resonance imaging. Prenatal Diagnosis, 2018, 38, 1035-1041.	2.3	7
59	Protocols for Harmonized Quantification and Noise Reduction in Low-Dose Oncologic 18F-FDG PET/CT Imaging. Journal of Nuclear Medicine Technology, 2019, 47, 47-54.	0.8	7
60	Automatic arm removal in PET and CT images for deformable registration. Computerized Medical Imaging and Graphics, 2006, 30, 469-477.	5.8	6
61	Impact on Image Noise of Incorporating Detector Blurring Into Image Reconstruction for a Small Animal PET Scanner. IEEE Transactions on Nuclear Science, 2009, 56, 2769-2776.	2.0	6
62	Patient body motion correction for dynamic cardiac <scp>PET</scp> â€ <scp>CT</scp> by attenuationâ€emission alignment according to projection consistency conditions. Medical Physics, 2019, 46, 1697-1706.	3.0	6
63	Evaluation of noise properties in PSF-based PET image reconstruction. , 2009, 2009, 3042-3047.		5
64	Limits of ultra-low dose CT attenuation correction for PET/CT. , 2009, 2009, 3074-3079.		5
65	Properties of edge artifacts in PSF-based PET reconstruction. , 2010, , .		5
66	Count-Rate Performance of the Discovery STE PET Scanner Using Partial Collimation. , 2006, 4, 2488-2493.		4
67	Consistency driven respiratory phase alignment and motion compensation in PET/CT. , 2007, 4, 3115-3119.		4
68	Pediatric chest CT radiation dose reduction: protocol refinement based on noise injection for pulmonary nodule detection accuracy. Clinical Imaging, 2013, 37, 334-341.	1.5	4
69	Performance Evaluation of Small Animal PET Scanners With Different System Designs. IEEE Transactions on Nuclear Science, 2013, 60, 1495-1502.	2.0	4
70	Relationships of Pediatric Anthropometrics for CT Protocol Selection. American Journal of Roentgenology, 2014, 203, W85-W91.	2.2	4
71	Spine Computed Tomography Radiation Dose Reduction. Spine, 2015, 40, 1613-1619.	2.0	4
72	Image Reconstruction for a Partially Collimated Whole Body PET Scanner. IEEE Transactions on Nuclear Science, 2008, 55, 975-983.	2.0	3

#	Article	IF	CITATIONS
73	Fast kVp-switching dual energy CT for PET attenuation correction. , 2009, , .		3
74	Noise and bias properties of monoenergetic images from DECT used for attenuation correction with PET/CT and SPECT/CT. , 2010, 7622, 762225-762228.		3
75	Blind analysis of CT image noise using residual denoised images. , 2015, , .		3
76	Fast analytical approach of application specific dose efficient spectrum selection for diagnostic CT imaging and PET attenuation correction. Physics in Medicine and Biology, 2016, 61, 7787-7811.	3.0	3
77	Improved attenuation correction for respiratory gated PET/CT with extended-duration cine CT: a simulation study. , 2017, , .		3
78	Quantitative myocardial perfusion from static cardiac and dynamic arterial CT. Physics in Medicine and Biology, 2018, 63, 105020.	3.0	3
79	PET/CT-guided biopsy with respiratory motion correction. International Journal of Computer Assisted Radiology and Surgery, 2019, 14, 2187-2198.	2.8	3
80	Sharing and Selling Images: Ethical and Regulatory Considerations for Radiologists. Journal of the American College of Radiology, 2021, 18, 298-304.	1.8	3
81	Improved quantitation for PET/CT image reconstruction with system modeling and anatomical priors. , 2005, , .		2
82	Estimating live-time for new PET scanner configurations. , 2007, 4, 2880-2884.		2
83	Direct reconstruction of CT-based attenuation correction images for PET with cluster-based penalties. , 2013, 2013, .		2
84	Assessment of patient selection criteria for quantitative imaging with respiratory-gated positron emission tomography. Journal of Medical Imaging, 2014, 1, 026001.	1.5	2
85	Simulation evaluation of quantitative myocardial perfusion assessment from cardiac CT. , 2014, 9033, 903303.		2
86	Evaluation of static and dynamic perfusion cardiac computed tomography for quantitation and classification tasks. Journal of Medical Imaging, 2016, 3, 024001.	1.5	2
87	Statistical distributions of ultra-low dose CT sinograms and their fundamental limits. , 2017, , .		2
88	Variable temporal sampling and tube current modulation for myocardial blood flow estimation from dose-reduced dynamic computed tomography. Journal of Medical Imaging, 2017, 4, 026002.	1.5	2
89	Technical Note: A digital reference object representing Hoffman's 3D brain phantom for PET scanner simulations. Medical Physics, 2020, 47, 1174-1180.	3.0	2
90	Constrain static target kinetic iterative image reconstruction for 4D cardiac CT imaging. , 2011, , .		1

#	Article	IF	CITATIONS
91	A digital reference object for the 3D Hoffman brain phantom for characterization of PET neuroimaging quality. , 2013, , .		1
92	Adaptive temporal smoothing of sinogram data using Karhunen-Loeve (KL) transform for myocardial blood flow estimation from dose-reduced dynamic CT. Proceedings of SPIE, 2014, , .	0.8	1
93	Statistical comparison of likelihood models for low dose x-ray CT. , 2014, , .		1
94	Comparison between pre-log and post-log statistical models in low-dose CT iterative reconstruction. , 2014, , .		1
95	Analysis of statistical models for iterative reconstruction of extremely low-dose CT data. , 2014, , .		1
96	Adaptive sampling of CT data for myocardial blood flow estimation from dose-reduced dynamic CT. Proceedings of SPIE, 2015, , .	0.8	1
97	Performance comparison between static and dynamic cardiac CT on perfusion quantitation and patient classification tasks. , 2015, , .		1
98	Application of big data analytics for automated estimation of CT image quality. , 2016, , .		1
99	Mixed Confidence Estimation for Iterative CT Reconstruction. IEEE Transactions on Medical Imaging, 2016, 35, 2005-2014.	8.9	1
100	Direct Reconstruction of CT-Based Attenuation Correction Images for PET With Cluster-Based Penalties. IEEE Transactions on Nuclear Science, 2017, 64, 959-968.	2.0	1
101	How to reconstruct dynamic cardiac PET data?. Journal of Nuclear Cardiology, 2017, 24, 291-293.	2.1	1
102	Use of Dual-Energy CT for Quantification of Essential Trace Metals (Iron, Copper, and Zinc): Proof of Concept. American Journal of Roentgenology, 2021, 216, 534-541.	2.2	1
103	Patient factors and outcomes associated with discordance between quantitative and qualitative cardiac PET ischemia information. PLoS ONE, 2021, 16, e0246149.	2.5	1
104	Comparison of models and acquisition techniques for estimation of myocardial blood flow from CT. Proceedings of SPIE, 2011, , .	0.8	0
105	Enhancing clinical utility of respiratory-gated PET/CT using patient respiratory trace classification. , 2012, , .		0
106	Vectorial total variation denoising for myocardial blood flow estimation in dynamic CT. , 2014, , .		0
107	A phantom design for assessment of detectability using a lumpy background and 3D-printed features. , 2015, , .		0
108	Evaluation of radiation dose reduction via myocardial frame reduction in dynamic cardiac CT for perfusion quantitation. , 2018, , .		0